

2017

An Investigation Into The Mechanism Of Cysteine-containing Thioredoxin Reductases: How Is Catalysis Conserved Without The Presence Of A Selenocysteine Residue?

Neil C. Payne
University of Vermont

Follow this and additional works at: <https://scholarworks.uvm.edu/hcoltheses>

Recommended Citation

Payne, Neil C., "An Investigation Into The Mechanism Of Cysteine-containing Thioredoxin Reductases: How Is Catalysis Conserved Without The Presence Of A Selenocysteine Residue?" (2017). *UVM Honors College Senior Theses*. 164.
<https://scholarworks.uvm.edu/hcoltheses/164>

This Honors College Thesis is brought to you for free and open access by the Undergraduate Theses at ScholarWorks @ UVM. It has been accepted for inclusion in UVM Honors College Senior Theses by an authorized administrator of ScholarWorks @ UVM. For more information, please contact donna.omalley@uvm.edu.

AN INVESTIGATION INTO THE MECHANISM OF CYSTEINE-CONTAINING
THIOREDOXIN REDUCTASES: HOW IS CATALYSIS CONSERVED WITHOUT
THE PRESENCE OF A SELENOCYSTEINE RESIDUE?

A Dissertation Presented

by

Neil Connor Payne

to

The Faculty of the College of Arts and Sciences

of

The University of Vermont

In Partial Fulfillment of the Requirements
For the Degree of Bachelor of Science
Specializing in Chemistry

April, 2017

Defense Date: April 27, 2017

Dissertation Examination Committee:

Robert J. Hondal, Ph.D., Advisor
Jay Silveira, Ph.D., Chair
Jose S. Madalengoitia, Ph.D.

Abstract

Thiorexodin reductase (TrxR) plays a major role in maintaining cellular antioxidant homeostasis. Mammalian TrxR (mTrxR) is defined by its rare, penultimate amino acid selenocysteine (Sec), which is essential to enzyme catalysis. However, some forms of TrxR in nature do not utilize Sec. One form of TrxR that does not use Sec is mitochondrial TrxR from *C. elegans* (CeTrxR2). Despite not possessing a Sec residue, CeTrxR2 maintains similar catalytic activity to mTrxR. It has been hypothesized that these Cys-containing TrxRs must somehow activate their active site C-terminal vicinal disulfide bond to achieve catalytic activity comparable to Sec-containing TrxRs, which instead contain a C-terminal vicinal selenosulfide bond. In order to further the understanding of how Cys-containing TrxRs maintain catalytic activity without the presence of Sec, we studied the mechanism of CeTrxR2 by synthesizing a mutant peptide substrate, whose activity towards a truncated form of CeTrxR2 was measured and compared with the wild-type peptide substrate. Our results provide evidence that a crucial hydrogen bond in the enzyme active site induces type VIa beta-turn formation, which places amino acid residues in the correct position for catalysis.

Dedication

To my Father and Mother, who have provided the most gracious support for me throughout not only my college years, but my entire life. I have and will continue to learn so much from both of you. Thank you for everything that you do.

Table of Contents

Abstract	2
Dedication	3
Table of Contents	4
List of Figures	6
List of Schemes	7
Chapter 1: Thioredoxin Reductase	8
1.1 Introduction	8
1.2 Previous Work Towards Understanding Cys-Containing TrxRs	13
1.3 Hypothesis: A Key Hydrogen Bond and Vicinal Disulfide Ring Conformation are Essential to CeTrxR Catalytic Activity.....	22
1.4 Plan to Test this Hypothesis	27
1.5 Retrosynthetic Analysis of Depsipeptide PRTQGCC(Gac).....	29
Chapter 2: Synthesis of Wild-Type and Mutant Peptides Corresponding to the C-Terminal Active Site of CeTrxR	31
2.1 Synthesis of Fmoc-Protected Cys(Mob)-Glycolic Acid Depside for Solid Phase Depsipeptide Synthesis.....	31
2.2 Synthesis of Mutant Depsipeptide 8-mer PRTQGCC(Gac) Corresponding to the C-terminal Active Site of CeTrxR	33
2.3 Synthesis of Wild Type Peptide 8-mer PRTQGCCG Corresponding to the C-terminal Active Site of CeTrxR.....	34

Chapter 3: Activity of Wild-Type and Mutant Peptide Substrates Towards	
Reduction by the N-terminal Redox Center of CeTrxRΔ8	35
3.1 Characterization and Assessment of Purity of PRTQGCCG and PRTQGCC(Gac)	
Substrates.....	35
3.2 Activity of Substrates Towards Reduction by CeTrxR Δ 8	41
Chapter 4: Summary and Future Directions	44
Chapter 5: Experimental Procedures	45
5.1 Materials and Methods	45
5.2 Synthetic Procedures	47

List of Figures

Figure 1	8
Figure 2	10
Figure 3	17
Figure 4	20
Figure 5	26
Figure 6	36
Figure 7	38
Figure 8	40
Figure 9	42
Figure 10	51
Figure 11	52
Figure 12	53
Figure 13	54
Figure 14	55
Figure 15	56
Figure 16	57
Figure 17	58

List of Schemes

Scheme 1	30
Scheme 2	32

Chapter 1: Thioredoxin Reductase

1.1 Introduction

Thioredoxin (Trx), thioredoxin reductase (TrxR) and NADPH constitute the thioredoxin system, which functions to maintain redox homeostasis in the cell and is ubiquitous from Archaea to *Homo sapiens*.¹ Trx is a small, 12 kDa enzyme of the oxidoreductase family and contains an active site dithiol that serves to catalyze the reduction of protein disulfides, its active site dithiol being oxidized to a disulfide in the process (**Figure 1**). Once oxidized, Trx serves as the native substrate for TrxR, which is a large, ~70 kDa dimeric protein and is a member of the family of the pyridine nucleotide-disulfide reductases. As such, TrxR can accept reducing equivalents in the form of NADPH through an enzyme bound FAD cofactor. These electrons then serve to reduce the N-terminal redox-active disulfide, which passes electrons to the enzyme's C-terminal redox center, which eventually transfers the electrons to Trx.

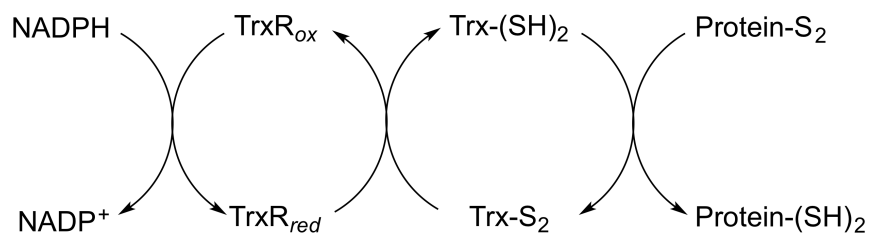


Figure 1. The thioredoxin system, composed of Trx, TrxR, and NADPH.

¹ Arnér, E. S. J.; Holmgren, A., Physiological functions of thioredoxin and thioredoxin reductase. *European Journal of Biochemistry* **2000**, 267 (20), 6102-6109.

The C-terminal active sites of many high M_r TrxRs contain the motif AA-Cys₁-X₂-AA, where X₂ can be either cysteine or, for many higher eukaryotes, selenocysteine (Sec), the rare, 21st amino acid. TrxR's C-terminal active site is also somewhat unique in that, when oxidized, its Cys₁/Cys₂ or Cys₁/Sec₂ residues form a vicinal disulfide/selenosulfide bond during the catalytic cycle.² Ultimately, it is this C-terminal disulfide/selenosulfide of TrxR that accepts electrons from the enzyme's N-terminal redox center and reduces Trx (see **Figure 2**).

In the case of mammalian (mTrxR) and rat (TrxR3) orthologs of TrxR, which contain selenium, it has been shown that the catalytic penultimate Sec residue is essential for catalysis.³ Specifically, it was showed that when the penultimate Sec residue was mutated to Cys, the k_{cat} of the mutant enzyme towards Trx was 175-fold lower than in the wild-type enzyme. Determination of the pH optimum of the mutant enzyme (pH 9) compared to the wild-type enzyme (pH 7) provided insight into why the Sec residue is so important for Sec-containing TrxRs. It is hypothesized that the lower pK_a of selenols when compared to thiols (pK_a = ~5.3 for Sec, pK_a = ~8.3 for Cys) must be important in the mechanism of action of TrxR, which likely relies on the superior nucleophilicity of a

² Carugo, O.; Čemažar, M.; Zahariev, S.; Hudáky, I.; Gáspári, Z.; Perczel, A.; Pongor, S., Vicinal disulfide turns. *Protein Engineering, Design and Selection* **2003**, *16* (9), 637-639.

³ Zhong, L.; Holmgren, A., Essential Role of Selenium in the Catalytic Activities of Mammalian Thioredoxin Reductase Revealed by Characterization of Recombinant Enzymes with Selenocysteine Mutations. *Journal of Biological Chemistry* **2000**, *275* (24), 18121-18128.

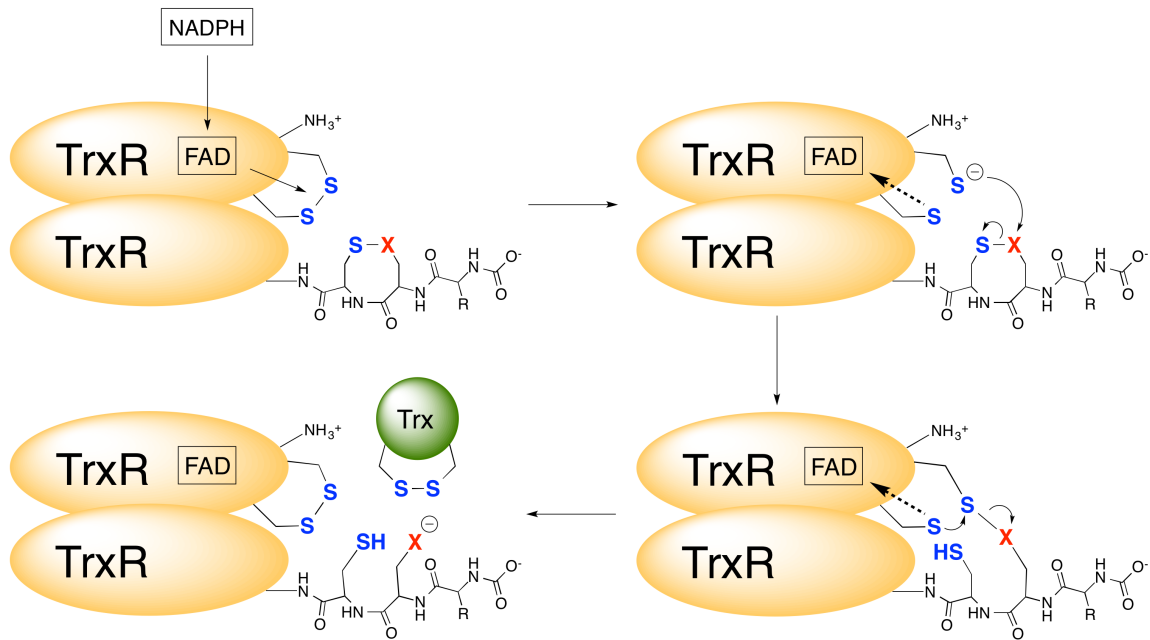


Figure 2. General mechanism of TrxR reduction. In the first step, NADPH transfers reducing equivalents through an FAD cofactor to the N-terminal redox center of one TrxR monomer. The resulting thiolate ion then attacks the C-terminal disulfide/selenosulfide (X = S or Se) of the other TrxR monomer, putting the C-terminal active site in a reduced form where it can reduce its native substrate, Trx.

Sec-selenolate anion when compared to a cysteine thiol.

Further studies by Hondal and coworkers elucidated another possible reason that selenium is essential for catalysis of Sec-containing TrxRs.⁴ The authors showed that when the positions of the C-terminal Cys and Sec residues were switched, the catalytic activity of the mutant enzyme dropped 100-fold. Moreover, they demonstrated that only Sec-containing TrxRs exhibit hydrogen peroxidase activity. Taken together, their results provided evidence that the unique chemical properties of the penultimate Sec residue are important for the mechanism of action of Sec-containing TrxRs, and that selenium is required for peroxidase activity.

While the various orthologs of TrxR that contain Sec are clearly dependent on the incorporation of selenium into the enzyme, there are other forms of TrxR in nature that do not use Sec. Some examples are TrxR from *Plasmodium falciparum* (PfTrxR)⁵, *Drosophila melanogaster* (DmTrxR)⁶, and mitochondrial TrxR from *Caenorhabditis*

⁴ Eckenroth, B. E.; Lacey, B. M.; Lothrop, A. P.; Harris, K. M.; Hondal, R. J., Investigation of the C-Terminal Redox Center of High-Mr Thioredoxin Reductase by Protein Engineering and Semisynthesis. *Biochemistry* **2007**, *46* (33), 9472-9483.

⁵ Gilberger, T.-W.; Bergmann, B.; Walter, R. D.; Müller, S., The role of the C-terminus for catalysis of the large thioredoxin reductase from *Plasmodium falciparum*. *FEBS Letters* **1998**, *425* (3), 407-410.

⁶ Gromer, S.; Johansson, L.; Bauer, H.; Arscott, L. D.; Rauch, S.; Ballou, D. P.; Williams, C. H.; Schirmer, R. H.; Arnér, E. S. J., Active sites of thioredoxin reductases: Why

elegans (CeTrxR2)⁷, which use a C-terminal motif containing a Cys-Cys dyad instead of Cys-Sec. It is then natural to ask the question: “how do orthologs of TrxR that do not use Sec maintain competent catalytic activity, given that replacement of Sec for Cys in Sec-containing TrxRs greatly diminishes catalysis?” This question provoked us to investigate the different mechanisms that Sec-absent TrxRs (termed Cys-containing TrxRs herein) use to perform their catalytic function. Specifically, the following dissertation outlines the starting point in an investigation aimed at addressing how CeTrxR2, the Cys-containing TrxR from *Caenorhabditis elegans*, managed to evolve without being dependent on Sec. It focuses on the synthesis and characterization of isosteric peptide fragments that correspond to the C-terminal active site of CeTrxR2. The project then transitions into the determination of peptide-disulfide reductase activity of these isosteric peptide fragments by the N-terminal redox center of CeTrxR2 by the employment of a truncated version of the enzyme (missing its terminal eight amino acid residues), with hopes of exposing a significant difference in this activity between the wild type and mutant peptides.

selenoproteins? *Proceedings of the National Academy of Sciences* **2003**, *100* (22), 12618-12623.

⁷ Lacey, B. M.; Hondal, R. J., Characterization of mitochondrial thioredoxin reductase from *C. elegans*. *Biochemical and Biophysical Research Communications* **2006**, *346* (3), 629-636.

1.2 Previous Work Towards Understanding Cys-Containing TrxRs

The first work aimed at addressing the question of how Cys-containing TrxRs compete with Sec-containing TrxRs was that of Arnér and coworkers⁶, where the authors hypothesized the importance of flanking serine residues towards the catalytic mechanism of DmTrxR (the C-terminal active site of DmTrxR contains a tetrapeptide -Ser-Cys-Cys-Ser-COOH motif). In this paper, it was shown that mutation of DmTrxR's C-terminal active site sequence to either -Gly-Cys-Cys-Gly-COOH or -Ser-Cys-Cys-Gly-COOH severely lowered the activity of the enzyme towards its native Trx substrate, however the -Gly-Cys-Cys-Ser-COOH mutation did not lose significant activity. Mutation of any of these sequences to contain Sec in the penultimate position did not result in any activity loss, even when both flanking residues were changed to Gly. Finally, mutation of the C-terminal sequence to contain either one or two flanking Asp residues diminished all activity of the resulting mutant enzymes. The combination of these results led the authors to hypothesize that the purpose of the flanking Ser residues in DmTrxR is to mediate thiolate formation during the catalytic cycle via hydrogen bonding, which lowers the effective pK_a s of the vicinal C-terminal cysteine residues. This lowering of pK_a would, as a result, increase their ability to perform thiol/disulfide exchange reactions more readily, as the thiolate anion is the more reactive form of sulfur (compared to a thiol).

These findings can be extended to provide a possible explanation of how the Cys-containing TrxR from *Anopheles gambiae* (AgTrxR) is an efficient catalyst without the

use of Sec⁸. AgTrxR contains a C-terminal active site sequence of –Thr-Cys-Cys-Ser-COOH and, thus, can also mediate thiolate formation via hydrogen bonds as hypothesized by Arnér and coworkers.⁶

In a subsequent study by Arnér and coworkers, it was shown that mutation of mTrxR's C-terminal active site (naturally –Gly-Cys-Sec-Gly-COOH) to mimic that of DmTrxR (with motif –Ser-Cys-Cys-Ser-COOH) caused the mutant enzyme to display <0.5% of wild-type enzyme activity.⁹ Using rapid kinetics studies, the authors showed that the transfer of reducing equivalents from the N-terminal disulfide/dithiol to the C-terminal active site disulfide/dithiol was much slower in the “DmTrxR-mimic” mutant enzyme compared to the wild-type enzyme. This led to the hypothesis that: “the active site microenvironment of DmTrxR must have been ‘fine-tuned’ in evolution to support the Ser-mediated activation of its active site Cys residues; alternatively, the features supporting such activation have been lost in the case of the mammalian enzyme.” These studies by Arnér provide strong evidence that the active site microenvironment of Cys-containing TrxRs is very important to the catalytic efficiency of these enzymes.

⁸ Bauer, H.; Gromer, S.; Urbani, A.; Schnölzer, M.; Schirmer, R. H.; Müller, H.-M., Thioredoxin reductase from the malaria mosquito *Anopheles gambiae*. *European Journal of Biochemistry* **2003**, *270* (21), 4272-4281.

⁹ Johansson, L.; Arscott, L. D.; Ballou, D. P.; Williams Jr, C. H.; Arnér, E. S. J., Studies of an active site mutant of the selenoprotein thioredoxin reductase: The Ser-Cys-Cys-Ser motif of the insect orthologue is not sufficient to replace the Cys-Sec dyad in the mammalian enzyme. *Free Radical Biology and Medicine* **2006**, *41* (4), 649-656.

Further illustrating the importance of the active site microenvironment of Cys-containing TrxRs, a study published by Hondal and coworkers demonstrated that when the C-terminal active site disulfide rings of DmTrxR and CeTrxR2 are mutated via insertion of Ala residues (in between the Cys residues), the activity of the mutant enzymes towards Trx dropped significantly (150-300-fold and 90-145-fold for DmTrxR and CeTrxR2, respectively, depending on how many Ala residues inserted).¹⁰ However, when Sec-containing mouse TrxR (mTrxR3) was mutated via the same procedure, only a modest 4-6 fold decrease in activity was observed.

These results are important for two reasons. First, they provided evidence for the hypothesis that Cys-containing TrxRs utilize ring strain⁶ to perform their catalytic function, as increasing the ring size of the C-terminal disulfide caused a decrease in activity to occur. Ring strain is present in this vicinal disulfide bond regardless of whether the peptide amide backbone adopts a *cis* or *trans* conformation.¹¹ In TrxRs that use Sec, this increase in ring size is not an issue due to the high electrophilicity of selenium in Sec, which accelerates the C-terminal active site's acceptance of electrons from the N-terminal redox center. Second, these results support a hypothesis set forth by Hondal and coworkers that the C-terminal vicinal disulfide ring of DmTrxR adopts a strained, *cis* amide bond conformation during the catalytic cycle to correctly place the

¹⁰ Eckenroth, B. E.; Lacey, B. M.; Lothrop, A. P.; Harris, K. M.; Hondal, R. J., Investigation of the C-Terminal Redox Center of High-Mr Thioredoxin Reductase by Protein Engineering and Semisynthesis. *Biochemistry* **2007**, *46* (33), 9472-9483.

¹¹ McMurray, J. (1988) *Organic Chemistry*, 2nd ed., p 173.

leaving group Cys thiolate anion near the acid-base catalytic His464' residue¹², which facilitates thiol/disulfide exchange¹³. This second point reiterates the significance of the C-terminal active site microenvironment for the maintenance of catalytic activity in Cys-containing TrxRs.

In another study by Hondal and coworkers, the authors demonstrated a major mechanistic difference between Cys- and Sec-containing TrxRs¹⁴. Truncated forms of mTrxR3, DmTrxR, and CeTrxR2 missing their last eight amino acid residues (mTrxR3 Δ 8, DmTrxR Δ 8, and CeTrxR2 Δ 8, respectively) were synthesized and assayed for activity towards oxidized peptide substrates corresponding to the C-terminal active sites of each enzyme. The key difference in the peptide substrates assayed was that some contained the native, *intrachain* vicinal disulfide/selenosulfide ring, while others contained an acyclic, *interchain* disulfide/selenosulfide bond, as shown in **Figure 3**. In the case of the interchain peptides, ring strain is relieved and the peptide is free to adopt energetically-favorable conformations.

¹² The ' denotes that this residue is present on the other monomer of the dimeric TrxR complex

¹³ Eckenroth, B. E.; Rould, M. A.; Hondal, R. J.; Everse, S. J., Structural and Biochemical Studies Reveal Differences in the Catalytic Mechanisms of Mammalian and *Drosophila melanogaster* Thioredoxin Reductases. *Biochemistry* **2007**, *46* (16), 4694-4705.

¹⁴ Lacey, B. M.; Eckenroth, B. E.; Flemer, S.; Hondal, R. J., Selenium in Thioredoxin Reductase: A Mechanistic Perspective. *Biochemistry* **2008**, *47* (48), 12810-12821.

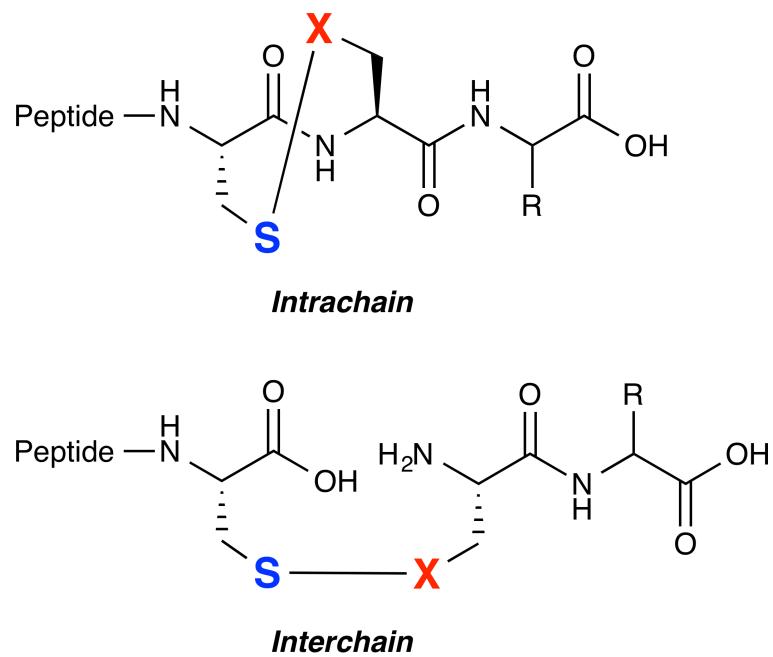


Figure 3. Intra- versus interchain peptides corresponding to the C-terminal active sites of TrxRs. Here, X can be either S or Se. This Figure was adapted from (14).

The results of assaying each truncated enzyme for reductase activity towards its corresponding intra- or interchain peptide showed that mTrxR3 Δ 8 (a native Sec-containing TrxR) only preferred the intrachain substrate over the interchain substrate by a factor of 32. However, DmTrxR Δ 8 and CeTrxR2 Δ 8 preferred their intrachain substrates by factors of 1025 and 2267, respectively. This led the authors to hypothesize that “only a special type of disulfide, a vicinal disulfide with *cis* amide geometry, can be a substrate for the truncated Cys-TR because only this type of disulfide has the right geometry to allow for thiolate attack by [the N-terminal redox center] while at the same time position the leaving group sulfur atom correctly to accept a proton from the general acid [His464’].” The relieving of the ring strain inherent in this *cis* amide geometry is also likely to play a role in Cys-containing TrxRs, as mentioned above.⁶

This hypothesis laid out by Hondal and coworkers was further evaluated in an in-depth study of Cys-containing DmTrxR.¹⁵ Like in their previous work¹⁴, the authors assayed truncated DmTrxR (DmTrxR Δ 8) for activity against wild-type and mutant peptide substrates corresponding to its native, C-terminal active site. However, this time the mutant peptides were varied from the wild-type substrate by increasing the vicinal disulfide ring size by one unit via the incorporation of homocysteine (hCys) residues, which contain an extra methylene group in their side chain. Their results showed that

¹⁵ Lothrop, A. P.; Snider, G. W.; Flemer, S.; Ruggles, E. L.; Davidson, R. S.; Lamb, A. L.; Hondal, R. J., Compensating for the Absence of Selenocysteine in High-Molecular Weight Thioredoxin Reductases: The Electrophilic Activation Hypothesis. *Biochemistry* **2014**, *53* (4), 664-674.

when the antepenultimate or penultimate Cys residue of the wild-type peptide was replaced by hCys (increasing the ring size to 9-membered from 8-membered), the N-terminal redox center of DmTrxR Δ 8 reduced the corresponding mutant disulfide ring slower by factors of 53 and 100, respectively. Interestingly, lipoic acid, a small molecule containing a strained, 5-membered disulfide ring, was a substrate for DmTrxR Δ 8 with only 11-fold less activity than the wild-type peptide substrate.

Mutant, full-length enzymes were also constructed where the antepenultimate (Cys₁), penultimate (Cys₂), or both Cys residues were replaced by hCys. When Cys₁ was mutated to hCys, the mutant enzyme displayed 240-fold less Trx reductase activity than the wild-type enzyme. However, when Cys₂ or both Cys residues were mutated to hCys, the mutant enzymes displayed only two-fold and 7-fold less activity than wild-type, respectively. An additional full-length, mutant enzyme was constructed where two Ala residues were inserted between the Cys₁-Cys₂ dyad, and this mutant displayed 300-fold less activity compared to the wild-type.

The combination of these results lead the authors to put forward a hypothesis that they term the “electrophilic activation hypothesis,” which is explained in **Figure 4**. This hypothesis ultimately takes into account all of the aforementioned data gathered on Cys-containing TrxRs, specifically DmTrxR, to suggest a mechanism of catalysis. The hypothesized mechanism demonstrates how any small change in the C-terminal active site microenvironment – whether it be varying ring strain, the interaction between specific residues, or effective pK_a values of cysteines – drastically affects the catalytic efficiency of Cys-containing TrxRs.

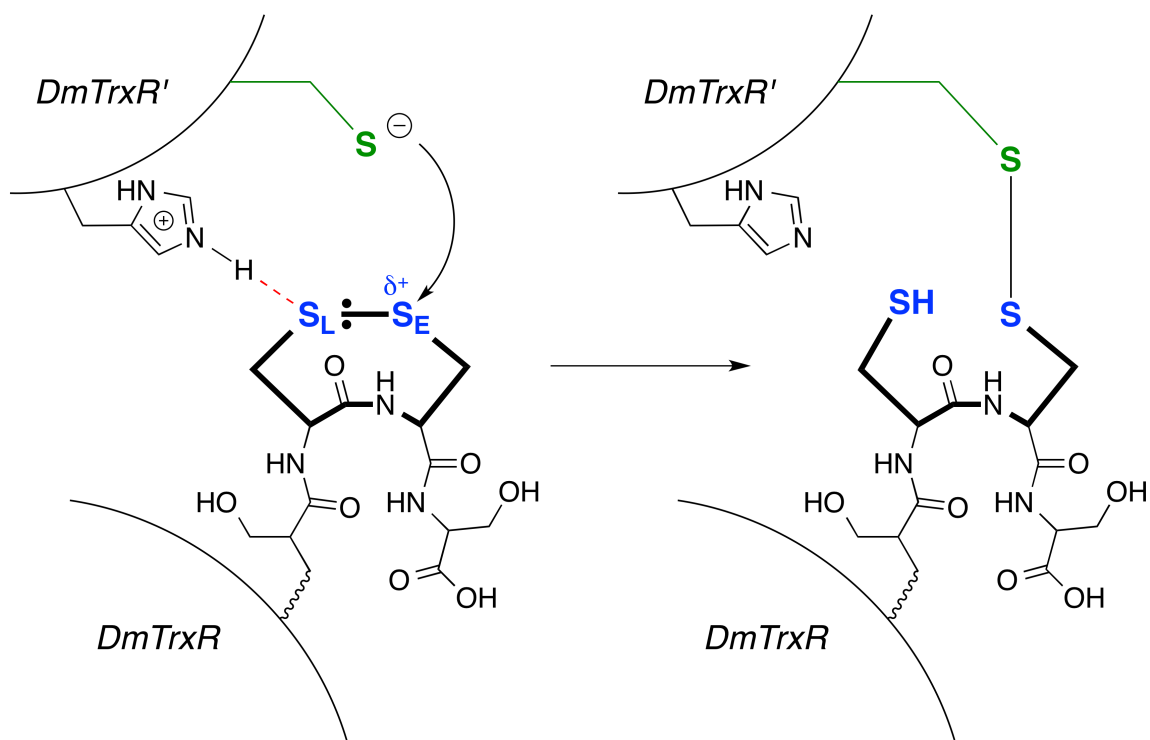


Figure 4. The “electrophilic activation hypothesis” explained. Hondal and coworkers hypothesize that the C-terminal vicinal disulfide bond of DmTrxR becomes polarized when the sulfur atom of Cys₁ (labeled S_L in the Figure) interacts with His464'H⁺. As a result, the sulfur of Cys₂ (labeled S_E in the Figure) becomes more electrophilic and is the acceptor of electrons during reduction by the N-terminal redox center (whose Cys-thiolate residue is shown in green). The leaving group thiolate (S_L) is then stabilized and protonated to form a thiol by the catalytic His464'H⁺ residue. This figure was adapted from (15).

While this hypothesized mechanism is an accurate model for the catalytic action of DmTrxR, it can be argued that the C-terminal active site microenvironment of CeTrxR2, which contains a –Gly-Cys-Cys-Gly-COOH motif instead of DmTrxR’s –Ser-Cys-Cys-Ser-COOH sequence, is different than the active site microenvironment of DmTrxR. It was previously shown that (i) the flanking Ser residues, especially the ultimate Ser residue, are essential to enzyme function and (ii) replacing these Ser residues with Gly (as in CeTrxR2) completely diminished Trx reductase activity.⁶ In addition, when comparing DmTrxR Δ 8 and CeTrxR2 Δ 8 activity towards their native C-terminal active site peptide 8-mers¹⁴, it was shown that CeTrxR2 Δ 8 preferred the “intrachain” substrate (see **Figure 3**) over the “interchain” substrate twice as much as DmTrxR Δ 8 preferred its own intrachain substrate. These findings give rise to the question of what different mechanism of action CeTrxR2 uses relative to DmTrxR, considering their different active site microenvironments yet shared independence of a Sec residue.

1.3 Hypothesis: A Key Hydrogen Bond and Vicinal Disulfide Ring Conformation are Essential to CeTrxR Catalytic Activity

In a 2007 study, Hondal and coworkers presented evidence that the conformation of the C-terminal vicinal disulfide ring of DmTrxR is important for catalytic activity.¹³ Their experiments were led by a key observation that TrxR, being in the family of pyridine nucleotide-disulfide oxidoreductases, can be seen as an extended version of glutathione reductase (GR) in which its C-terminus is the substrate, contrary to GR where oxidized glutathione (GSSG) is the substrate. With this idea in mind, the authors determined which conformations of the peptide fragment –Ser-Cys-Cys-Ser-COOH (SCCS_{ox}), which corresponds to the C-terminal active site of DmTrxR, *aligned with* GSSG in the active site binding pocket of the enzyme (determined from X-ray crystallography). Their results showed that the sulfur atoms of SCCS_{ox} aligned with those of GSSG when the conformation of the Cys-Cys amide bond was *cis*. Furthermore, this *cis* conformation placed the leaving group Cys residue in the right position to accept a proton from His464'H⁺, which should theoretically facilitate thiol-disulfide exchange between the N-terminal and C-terminal redox centers of DmTrxR.

Given that this active site His residue is conserved among GR¹⁶ and all

¹⁶ Rietveld, P.; Arscott, L. D.; Berry, A.; Scrutton, N. S.; Deonarain, M. P.; Perham, R. N.; Williams, C. H., Reductive and oxidative half-reactions of glutathione reductase from *Escherichia coli*. *Biochemistry* **1994**, *33* (46), 13888-13895.

TrxRs¹⁷ as an acid-base catalyst, it can be hypothesized that this *cis* amide bond conformation is important for how another Cys-containing TrxR, CeTrxR2, performs catalysis. Due to the lack of flanking Ser residues (as in DmTrxR) to the oxidized Cys-Cys dyad in CeTrxR2, this requirement for specific conformation of active site amino acid residues is likely even more important for CeTrxR2 than it is for DmTrxR.

Up until this point, it has been reiterated that all Cys-containing TrxRs form a vicinal disulfide ring between adjacent C-terminal Cys residues. It should be pointed out, however, that this type of disulfide ring is found in only ~50 protein data bank (PDB) structures¹⁸, and in almost every case it has been shown that they impart an important enzymatic role.¹⁹ In enzymes, this [Cys-Cys]_{ox} dyad is part of a two residue turn that can fit the molecular constraints of types I, II, VIa, VIb, and VIII β -turns.¹⁸ Types VIa and VIb are unique in that the amide bond between residues ($i + 1$) and ($i + 2$) – the amide

¹⁷ Gromer, S.; Wessjohann, L. A.; Eubel, J.; Brandt, W., Mutational Studies Confirm the Catalytic Triad in the Human Selenoenzyme Thioredoxin Reductase Predicted by Molecular Modeling. *ChemBioChem* **2006**, 7 (11), 1649-1652.

¹⁸ Hudáky, I.; Gáspári, Z.; Carugo, O.; Čemažar, M.; Pongor, S.; Perczel, A., Vicinal disulfide bridge conformers by experimental methods and by ab initio and DFT molecular computations. *Proteins: Structure, Function, and Bioinformatics* **2004**, 55 (1), 152-168.

¹⁹ Avizonis, D. Z.; Farr-Jones, S.; Kosen, P. A.; Basus, V. J., Conformations and Dynamics of the Essential Cysteinyl-Cysteine Ring Derived from the Acetylcholine Receptor. *Journal of the American Chemical Society* **1996**, 118 (51), 13031-13039.

bond between adjacent Cys residues in the case of TrxR – adopts a *cis* orientation rather than *trans*. While isomerization of this amide bond and subsequent β -turn constraint can occur spontaneously, type VIa and VIb β -turns possess NH($i + 3$)-CO(i) hydrogen bonds that help to stabilize the *cis* orientation of the ($i + 1$)-($i + 2$) amide bond.²⁰

By integrating the data from Hondal and coworkers¹³ with the idea of the [Cys-Cys]_{ox} dyad in CeTrxR2 forming a VIa or VIb β -turn (with *cis* amide geometry), it can be hypothesized that the NH($i + 3$)-CO(i) hydrogen bond stabilizes the *cis* amide bond conformation of the β -turn. Removal of this hydrogen bond should favor spontaneous *cis/trans* isomerization, allowing the dyad to adopt the multiple other different β -turn constraints described above. Therefore, if a mutant enzyme of CeTrxR2 is constructed so that the C-terminal NH($i + 3$)-CO(i) hydrogen bond is removed, it would be expected that catalysis would be greatly diminished because (i) ring strain would be relieved, as the [Cys-Cys]_{ox} dyad would adopt a lower energy, *trans* amide bond conformation, and (ii)

²⁰ (i) Ishimoto, B.; Tonan, K.; Ikawa, S.-i., Coupling of intramolecular hydrogen bonding to the *cis*-to-*trans* isomerization of a proline imide bond of small model peptides.

Spectrochimica Acta Part A: Molecular and Biomolecular Spectroscopy **2000**, *56* (1), 201-209. (ii) Sugawara, M.; Tonan, K.; Ikawa, S.-i., Effect of solvent on the *cis*-*trans* conformational equilibrium of a proline imide bond of short model peptides in solution.

Spectrochimica Acta Part A: Molecular and Biomolecular Spectroscopy **2001**, *57* (6),

1305-1316. (iii) Meng, H. Y.; Thomas, K. M.; Lee, A. E.; Zondlo, N. J., Effects of i and $i+3$ residue identity on *Cis*-*Trans* isomerism of the aromatic $i+1$ -prolyl $i+2$ amide bond:

Implications for type VI β -turn formation. *Peptide Science* **2006**, *84* (2), 192-204.

isomerization of the $(i + 1)$ - $(i + 2)$ amide bond to the *trans* conformation would place the leaving group Cys residue in an incorrect position to accept a proton from His464'H⁺. Removal of the NH $(i + 3)$ -CO (i) hydrogen bond can be accomplished by replacing the conventional $(i + 3)$ amide bond with an isosteric ester bond. This hypothesis is further explained in **Figure 5**.

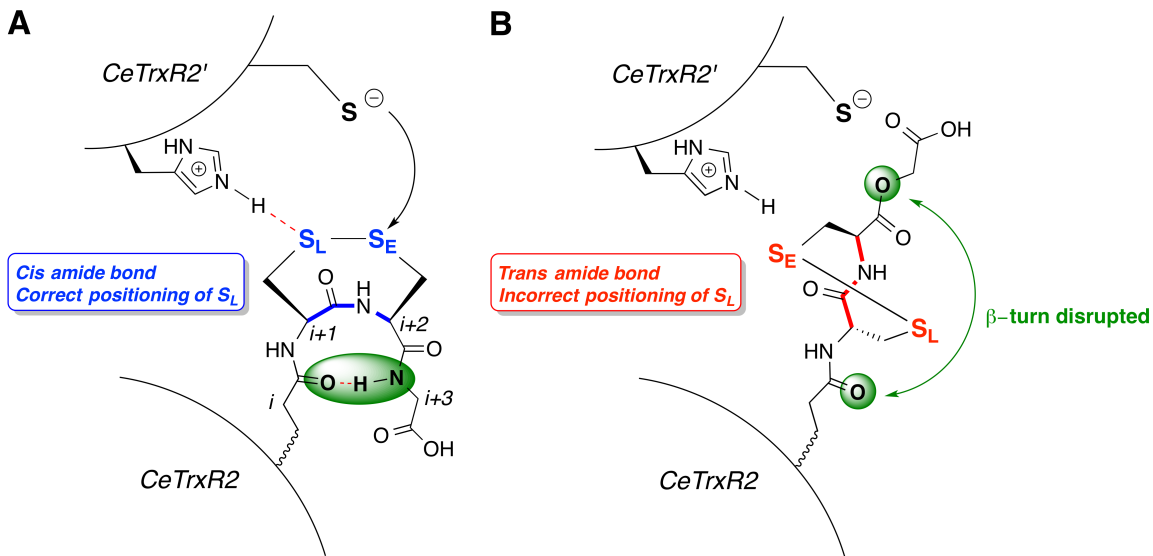


Figure 5. (A) In the wild-type CeTrxR2, the NH($i + 3$)-CO(i) hydrogen bond (shown in green) stabilizes the *cis* amide bond conformation and concomitant type VIa/VIb β -turn, which places the leaving group Cys sulfur atom (S_L) in the correct position to accept a proton from His464' H^+ . (B) If the native ($i + 3$) amide bond is replaced with an isosteric ester bond, then this hydrogen bonding cannot occur. As a result, the β -turn will be disrupted because the *trans* amide bond conformation will be preferred, which will cause incorrect positioning of S_L towards His464' H^+ . This loss of active site cooperation should result in a substantial decrease in the catalytic abilities of the mutant enzyme.

1.4 Plan to Test this Hypothesis

The goal of this work is to first construct peptide 8-mers that correspond to both the wild-type C-terminal active site of CeTrxR2 (PRTQGCCG) and the mutant C-terminal active site containing an ultimate ester linkage, in which the last amino acid (glycine) has been replaced by glycolic acid (PRTQGCC(Gac)).²¹ Next, these peptide fragments will be assayed for activity towards a truncated version of CeTrxR2 that is missing its last eight C-terminal amino acid residues (CeTrxR Δ 8).¹⁴ This assay will assess the N-terminal redox center's ability to reduce the wild-type and mutant peptide substrates. By comparing the rate of peptide turnover (wild-type versus mutant) by the N-terminal redox center, a conclusion may be drawn as to the importance of the NH(i + 3)-CO(i) hydrogen bond for catalysis. If the mutant peptide that cannot form this hydrogen bond shows no decrease in activity towards CeTrxR Δ 8, then the result will be interpreted as: the C-terminal active site shows no preference for the conformation of the amide backbone. However, if a large decrease in activity is observed, then the result will be interpreted as the opposite: the enzyme *does* utilize a stabilizing hydrogen bond to adopt a strained, *cis* amide bond conformation (and concomitant type VIa/VIb β -turn) that places the leaving group Cys sulfur atom in the correct position to abstract a proton from His464'H⁺, as described in **Figure 5**.

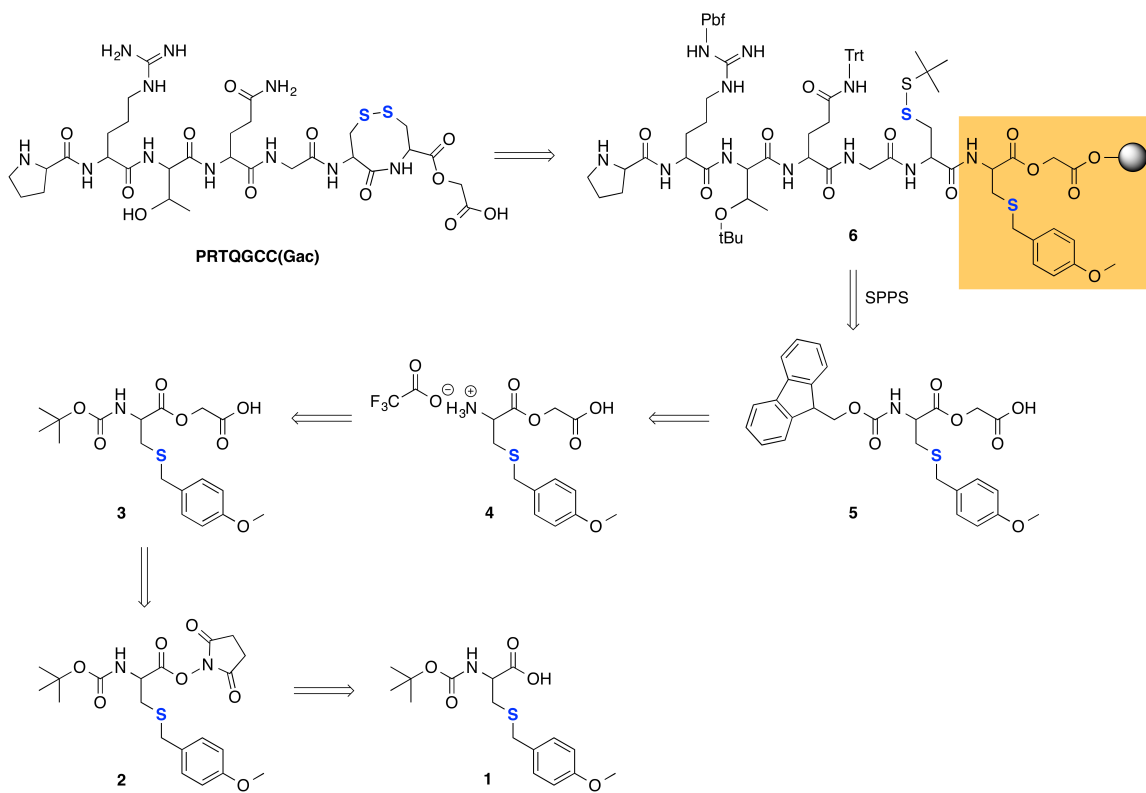
²¹ The mutant 8-mer cannot be synthesized by normal solid phase peptide synthesis (SPPS) protocol; the retrosynthetic analysis of the mutant peptide is discussed in **Chapter 1.5**.

While it is not the primary focus of this work, the next step towards understanding the importance of this hydrogen bond will be evaluated by constructing a full length, mutant enzyme that contains an ultimate ester linkage between the penultimate Cys residue and glycolic acid. Once constructed, the wild-type and full length enzymes will be assayed for Trx reductase activity. The results of this assay would be interpreted the same way as described in the previous paragraph.

1.5 Retrosynthetic Analysis of Depsipeptide PRTQGCC(Gac)

A retrosynthetic analysis of the mutant depsipeptide containing an ester linkage between the penultimate cysteine residue and ultimate glycolic acid residue was proposed (**Scheme 1**). Starting from commercially available Boc-S-(4-methoxybenzyl)-L-cysteine (**1**), we envisioned activating the carboxylic acid residue via a DCC coupling to *N*-hydroxysuccinimide to form succinimide ester **2**. Esterification with glycolic acid using pyridine and catalytic 4-dimethylaminopyridine (DMAP) would yield the Boc-protected Cys(Mob)-glycolic acid depside **3**. Deprotection of Boc with 1:1 TFA/DCM could give TFA salt **4**. Finally, subsequent protection with Fmoc-OSu would yield the solid phase peptide synthesis (SPPS)-compatible depside **5**, whose carboxyl group could be directly coupled to 2-chlorotrityl chloride resin. The remaining six amino acids could be attached via conventional SPPS methods to yield protected depsipeptide **6** linked to 2-chlorotrityl chloride resin. Finally, simultaneous deprotection and cleavage of **6** from resin²² would yield mutant depsipeptide PRTQGCC(Gac) containing the necessary vicinal disulfide ring, which may be reduced by the N-terminal active site of CeTrxRΔ8.

²² Flemer Jr, S.; Lacey, B. M.; Hondal, R. J., Synthesis of peptide substrates for mammalian thioredoxin reductase. *Journal of Peptide Science* **2008**, *14* (5), 637-647.

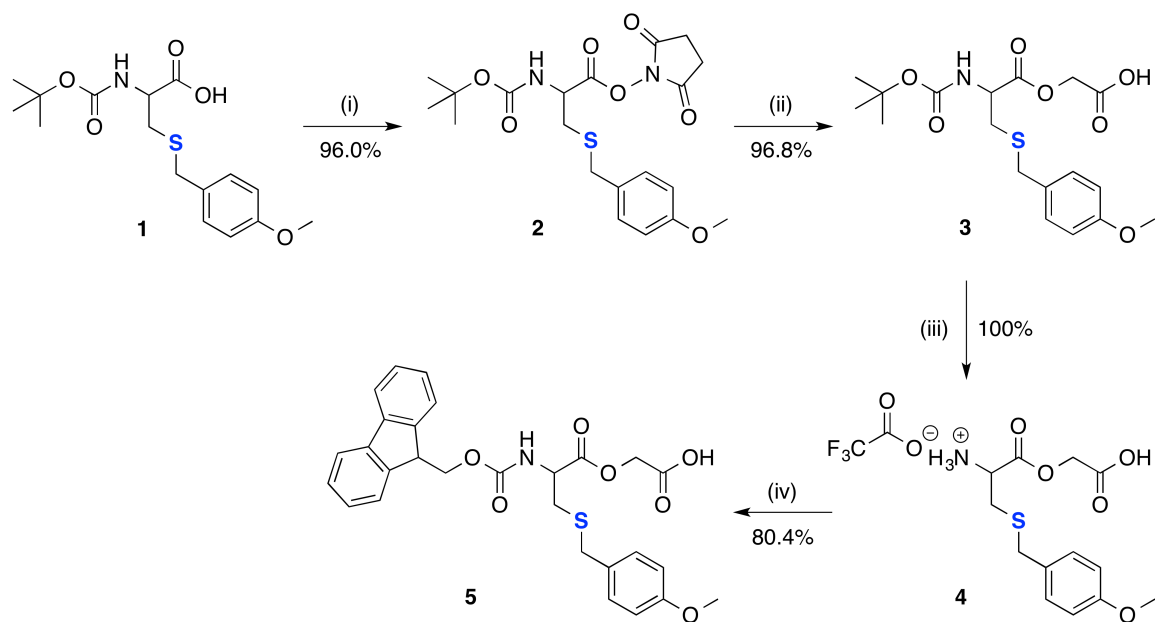


Scheme 1. Retrosynthetic toward mutant depsipeptide PRTQGCC(Gac).

Chapter 2: Synthesis of Wild-Type and Mutant Peptides Corresponding to the C-Terminal Active Site of CeTrxR

2.1 Synthesis of Fmoc-Protected Cys(Mob)-Glycolic Acid Depside for Solid Phase Depsipeptide Synthesis

Employing a DCC coupling reaction between starting material **1** and *N*-hydroxysuccinimide afforded Boc-protected succinimide ester **2** in 96.0% yield (**Scheme 2**). Esterification with glycolic acid proceeded smoothly in the presence of pyridine and DMAP to give depside **3** in 96.8% yield. The Boc protecting group was removed via treatment with 1:1 TFA/DCM, which upon evaporation of solvent followed by repeated solvation and evaporation by methanol (to remove residual TFA) yielded pure TFA salt **4** (100% yield assumed). TFA salt **4** was used without further purification in a reaction with Fmoc-Osu under basic conditions in a mixture of H₂O/dioxane to afford Fmoc-protected depside **5** in 80.4% yield after purification on SiO₂.



Scheme 2. Synthesis of Fmoc-protected depside (**5**). Reaction conditions: (i) N-hydroxysuccinimide, DCC, ACN, inert atmosphere, 0 °C → r.t., 24 h; (ii) glycolic acid, pyridine, DMAP, THF, reflux, 24 h; (iii) 1:1 TFA/DCM, 1 h; (iv) Fmoc-OSu, NaHCO₃, H₂O/dioxane, 0 °C → r.t., 24 h.

2.2 Synthesis of Mutant Depsipeptide 8-mer PRTQGCC(Gac) Corresponding to the C-terminal Active Site of CeTrxR

The initial reaction coupling depside **5** to 2-chlorotrityl chloride resin was carried out using *N*-methylmorpholine (NMM) in DCM. Coupling using standard Fmoc deprotection and HATU activation was employed for peptide elongation. Once the N-terminal proline residue was coupled to the peptide, the α -Fmoc protecting group was converted to Boc first by treating the resin with 20% piperidine in DMF, followed by incubation with Boc anhydride and NMM in 1:1 DMF/DCM. The removal of the S-tBu protecting group from Cys was accomplished by treating the resin with 20% β -mercaptoethanol (β -ME) in DMF. The deprotected Cys residue was then activated by reaction with 2,2'-dithiobis(5-nitropyridine) (DTNP) to form the 5-Npys conjugate. Deprotection, cyclization, and cleavage of the depsipeptide from the resin was achieved by incubating the resin with 94:2:2:2 TFA/TIS/H₂O/thioanisole. The crude depsipeptide mixture was precipitated into cold, anhydrous diethyl ether. The resulting solid was spun into a pellet, dissolved in water, frozen, and lyophilized to yield fully deprotected PRTQGCC(Gac).

2.3 Synthesis of Wild Type Peptide 8-mer PRTQGCCG Corresponding to the C-terminal Active Site of CeTrxR

The synthesis of the wild-type peptide PRTQGCCG followed the same procedure for the synthesis of the mutant peptide PRTQGCC(Gac), except the initial amino acid coupling to 2-chlorotrityl chloride resin used glycine instead of depside **5**. The remaining 7 amino acids were then attached using standard Fmoc deprotection and HATU activation protocols as described in **Chapter 2.2**.

Chapter 3: Activity of Wild-Type and Mutant Peptide Substrates Towards Reduction by the N-terminal Redox Center of CeTrxR Δ 8

3.1 Characterization and Assessment of Purity of PRTQGCCG and PRTQGCC(Gac) Substrates

The mass spectra of the wild-type PRTQGCCG and mutant PRTQGCC(Gac) peptide substrates synthesized by SPPS are shown in **Figure 6**. The mass spectrum of PRTQGCCG shows the main ionization form of PRTQGCCG is the doubly-charged, (M + 2H)²⁺ state with $m/z = 410.3$, which is attributable to the highly basic α -amine and arginine-guanidinium functionalities of the peptide substrate. Similarly, in the mass spectrum of PRTQGCC(Gac), the main ionization state of PRTQGCC(Gac) was (M + 2H)²⁺ with $m/z = 410.8$. However, unlike in the mass spectrum of PRTQGCCG where the peptide $m/z = 410.3$ was the ion with the greatest intensity, in the mass spectrum of PRTQGCC(Gac) the ion with the greatest intensity was $m/z = 280.3$. This m/z value could not be readily identified.

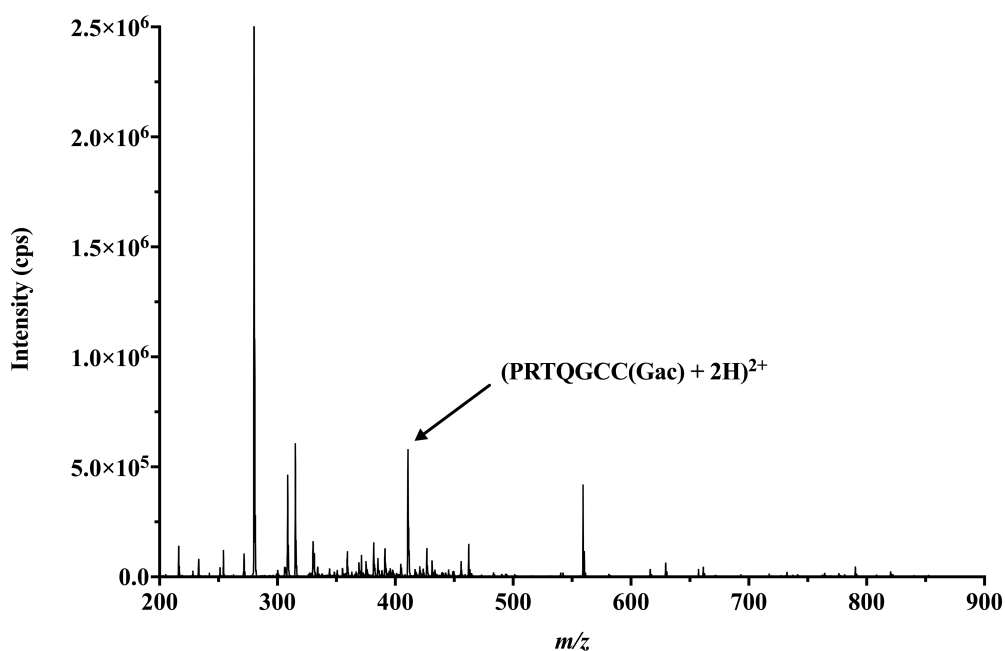
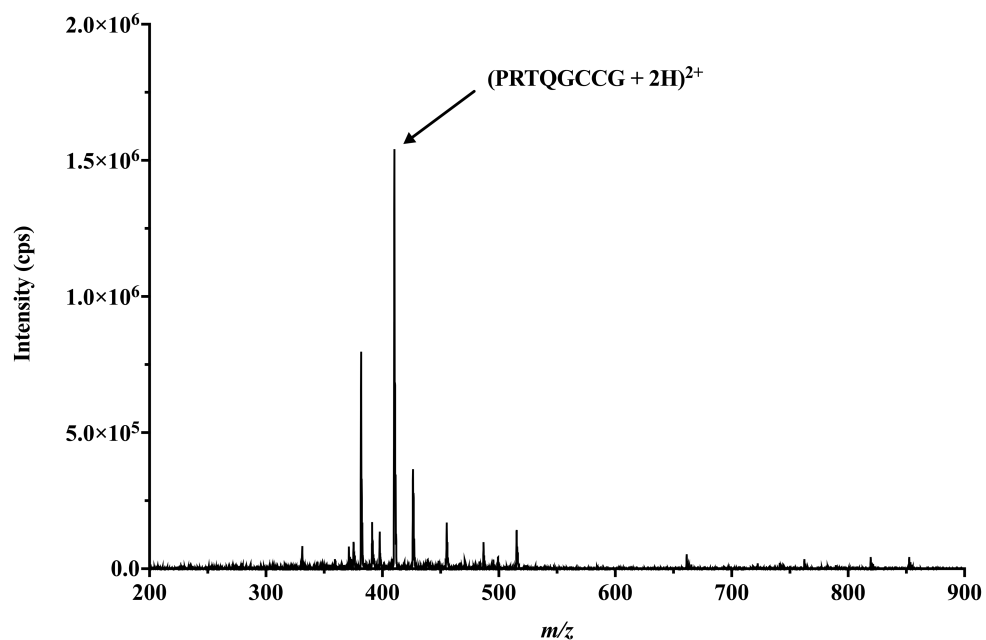


Figure 6. (top) Mass spectrum of wild-type peptide PRTQGCCG. The main ionization form of PRTQGCCG is the doubly-charged, $(M + 2H)^{2+}$ state with $m/z = 410.3$. (bottom) Mass spectrum of mutant peptide PRTQGCC(Gac). Similarly, the main ionization form of PRTQGCC(Gac) is the doubly-charged, $(M + 2H)^{2+}$ state with $m/z = 410.8$.

In an effort to assess the purity of each substrate, each peptide sample was subjected to HPLC analysis. **Figure 7** shows the HPLC traces of 50 μ L injections of 2.44 mM solutions of either PRTQGCCG (red trace) or PRTQGCC(Gac) (blue trace) in 100 mM potassium phosphate buffer, pH 7.0. In both cases, elutions possessing retention times of less than 5 min corresponded to the elution of phosphate buffer. The HPLC traces show that each peptide sample contained significant impurities.

The identity of each eluting peak cannot be assumed in routine HPLC experiments. As such, aliquots of each solution were subjected to HPLC-MS analysis (data not shown). The extracted ion chromatograms (EIC) monitoring the elution of m/z values corresponding to either PRTQGCCG or PRTQGCC(Gac) showed that, in each case, the peptide 8-mers possessed the shortest respective retention times in each chromatogram, apart from potassium phosphate elution.

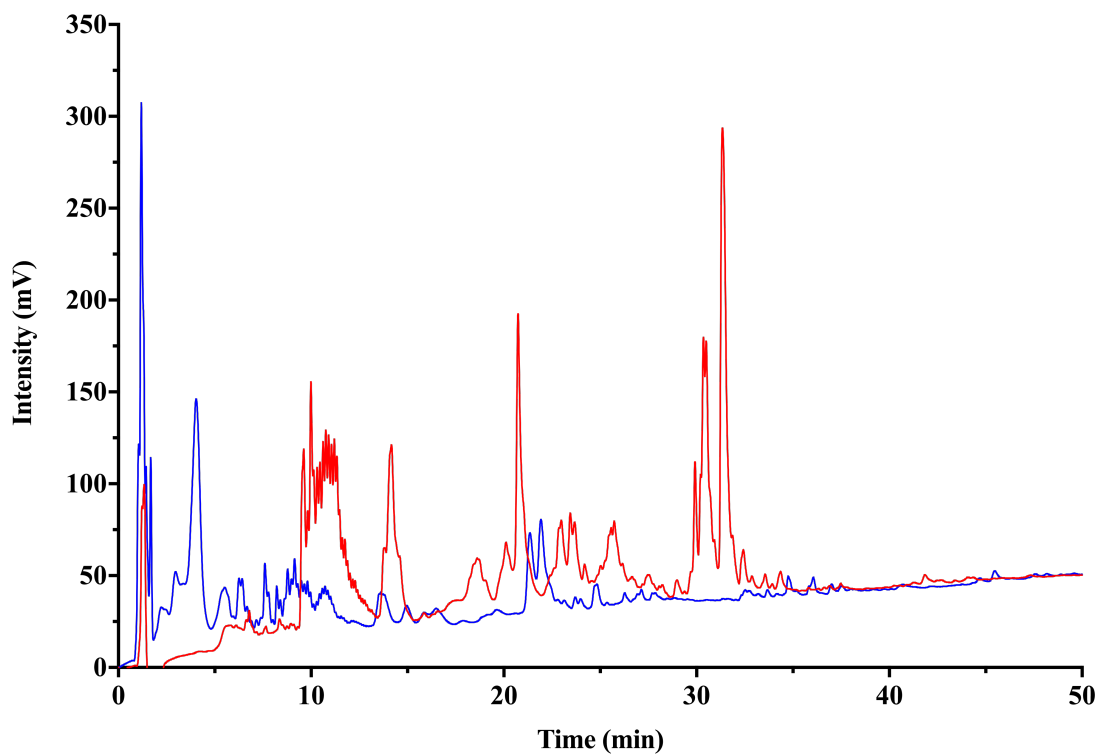


Figure 7. HPLC traces of PRTQGCCG (red) and PRTQGCC(Gac) (blue) samples. HPLC analyses were conducted by injecting 50 μ L of 2.44 mM solutions of either PRTQGCCG or PRTQGCC(Gac) in 100 mM potassium phosphate buffer, pH 7.0.

Considering this fact, it was hypothesized that PRTQGCCG (red trace) and PRTQGCC(Gac) (blue trace) eluted from the HPLC column with retention times of 9.5-13.3 min and 8.3-11.7 min, respectively, as illustrated in **Figure 8**. The detector utilized in this HPLC experiment measured the absorbance at $\lambda = 214$ nm, rendering Beer's Law applicable. As such, it was hypothesized that the effective concentration of PRTQGCCG in the respective peptide sample was approximately 3 times greater than the effective concentration of PRTQGCC(Gac), judging from the area of each elution peak.

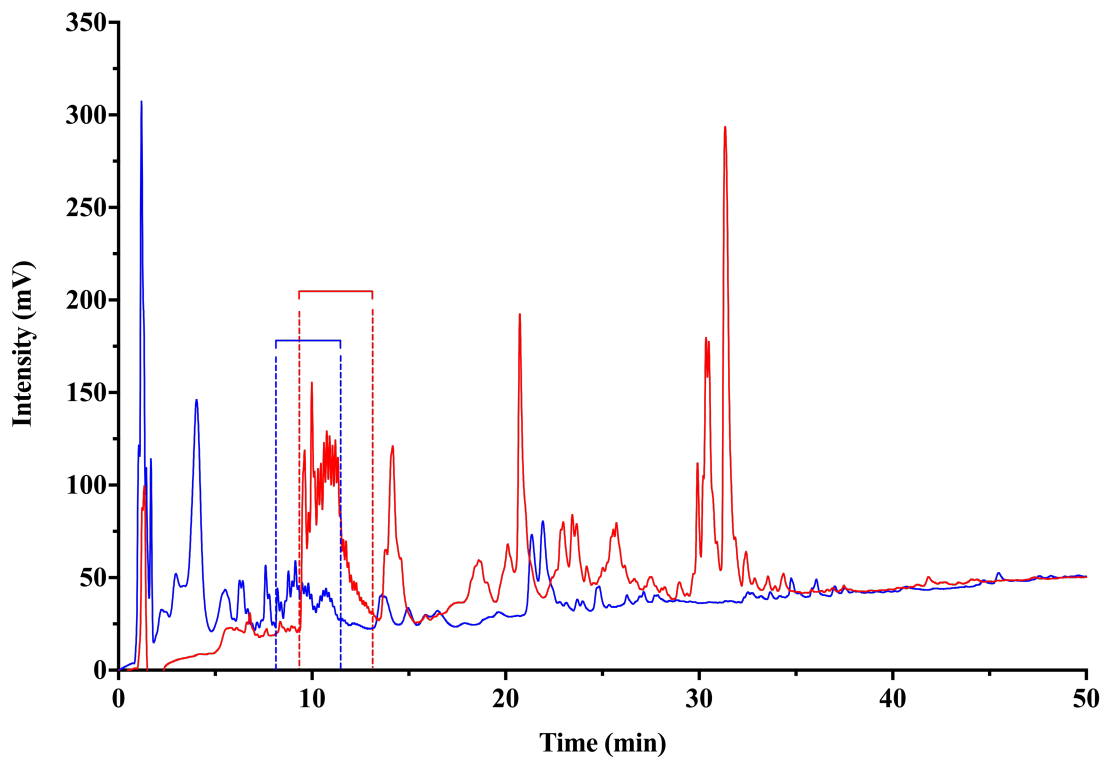


Figure 8. Possible elution profiles of PRTQGCCG (red trace) and PRTQGCC(Gac) (blue trace). Based on HPLC-MS and resulting EIC data, it was hypothesized that PRTQGCCG eluted from the HPLC column with a retention time of 9.5-13.3 min (red dashed lines), while PRTQGCC(Gac) eluted from the column at 8.3-11.7 min (blue dashed lines). HPLC analyses were conducted by injecting 50 μ L of 2.44 mM solutions of either PRTQGCCG or PRTQGCC(Gac) in 100 mM potassium phosphate buffer, pH 7.0.

3.2 Activity of Substrates Towards Reduction by CeTrxR Δ 8

Assaying both the wild-type and mutant peptide substrates for activity towards a truncated form of CeTrxR that is missing its last eight amino acid residues (CeTrxR Δ 8) allows conclusions to be drawn with respect to the N-terminal redox center's ability to reduce the vicinal disulfide ring present on each peptide. In the full-length enzyme possessing these last eight amino acids, this vicinal disulfide ring would be present between the antepenultimate and penultimate cysteine residues and can be reduced by the N-terminal redox center of the enzyme. Therefore, if the reductive activity of the mutant peptide by CeTrxR Δ 8 is lower or higher than that of the wild-type peptide, the result will be interpreted as both the NH(i+3)-CO(i) hydrogen bond and concomitant type VIa β -turn conformational preference being either important or not important for catalytic activity of CeTrxR.

The CeTrxR Δ 8 reductase activity towards both the wild-type and mutant peptide substrates is shown in a Michaelis-Menten plot in **Figure 9**. The Figure shows a dramatic difference in the activity of CeTrxR Δ 8 towards each substrate. While the activity of CeTrxR Δ 8 towards the wild-type peptide PRTQGCCG steadily increases with increasing peptide concentration, the opposite is true for the mutant depsipeptide PRTQGCC(Gac): the truncated enzyme's activity towards the mutant substrate is identical to the inherent background NADPH oxidase activity of CeTrxR Δ 8.

While these data seem to support the central hypothesis that the NH(i+3)-CO(i) hydrogen bond and concomitant type VIa β -turn conformational preference play a vital role in catalysis of CeTrx2, this result must be taken with caution. In **Figure 7** and

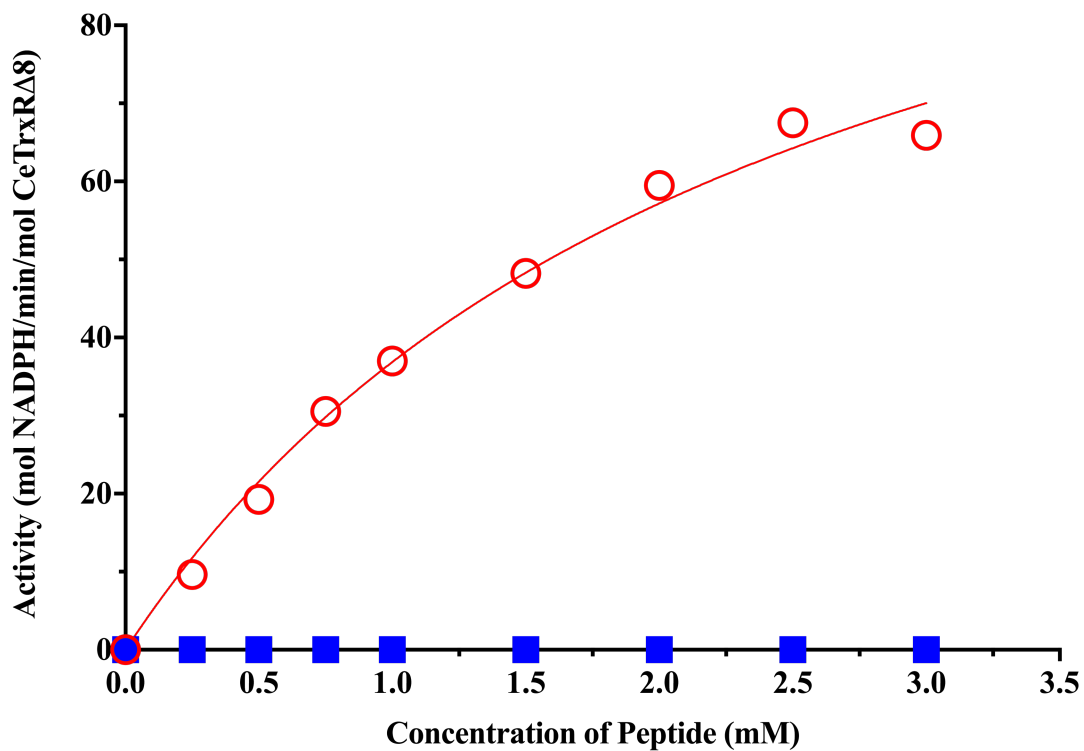


Figure 9. Activity of CeTrxRA8 towards PRTQGCCG (wild-type, blue bars) and PRTQGCC(Gac) (mutant, red bars) peptide substrates. The activity was monitored by consumption of NADPH via a decrease in absorbance at 340 nm. Reaction mixtures contained 100 mM potassium phosphate, pH 7.0, 1 mM EDTA, 200 μ M NADPH, 0.25-3.00 mM peptide, and 100 nM CeTrxRA8. The wild-type peptide is represented by the red open circles (PRTQGCCG), blue closed squares represent the mutant peptide (PRTQGCC(Gac)).

Figure 8, attention was brought to the fact that the peptide samples used in this assay were (i) not entirely pure and (ii) possessed what seemed to be different effective concentrations of the correct peptide substrates. Therefore, the possibility arises that this decrease in activity may be attributed to there being less peptide substrate present in the mutant peptide assay. In further studies, the crude peptide samples must be purified in order to rule this possibility out.

Chapter 4: Summary and Future Directions

In summary, wild-type (PRTQGCCG) and mutant (PRTQGCC(Gac)) peptide substrates were synthesized and their purity was assessed. Each peptide sample contained significant impurities as shown in the HPLC traces in **Figure 7**. In addition, each peptide sample may have possessed unequal effective concentrations of the relevant peptide substrate to be reduced by the truncated form of CeTrxR2 missing its last 8 amino acid residues (CeTrx2 Δ 8). When the peptide substrates were assayed against CeTrx2 Δ 8, the mutant peptide displayed no detectable activity. This result may support the hypothesis that the NH(i+3)-CO(i) hydrogen bond and concomitant type VIa β -turn conformational preference play a vital role in catalysis of CeTrx2.

In future studies, the peptide substrates must be purified before they are assayed for activity against CeTrx2 Δ 8. In addition, a full length, mutant enzyme that contains an ultimate ester linkage between the penultimate Cys residue and glycolic acid must be constructed. The wild-type and full length mutant enzymes should be assayed for Trx reductase activity.

Chapter 5: Experimental Procedures

5.1 Materials and Methods

Unless otherwise stated, all non-aqueous reactions were carried out in either oven-dried or flame-dried glassware. All commercially available starting materials were purchased from Aldrich, Fischer Scientific, or Acros Organics, and used as received. Analytical TLC was performed on Millipore TLC Silica gel 60 F₂₅₄ silica gel plates with UV indicator. Visualization was accomplished by irradiation under a 254 nm UV lamp or stained with either an aqueous solution of CAM, KMnO₄, or phosphomolybdic acid. Flash chromatography was performed using a forced flow of the indicated solvent system on Select Scientific Silica Gel (32-63 particle size). Removal of solvents was accomplished on a Büchi R-114 rotary evaporator and compounds were further dried under a high vacuum line.

All ¹H data was conducted at ambient temperatures and recorded on a Varian UnityInova (500 MHz) or Bruker ARX (500 MHz) spectrometer. ¹³C NMR spectra were recorded on a Bruker ARX (125 MHz) spectrometer. Chemical shifts are reported relative to chloroform ($\delta = 7.27$) for ¹H spectra and chloroform ($\delta = 77.2$) for ¹³C spectra. Data are reported as follows: chemical shift, multiplicity (s = singlet, d = doublet, t = triplet, q = quartet, p = pentet, br = broad, m = multiplet), coupling constants (Hz), and number of protons. Direct infusion mass spectrometry was executed using an ABI Sciex 4000QTrap Pro LCMS in positive-ESI mode. Liquid chromatography-mass spectrometry was executed using an ABI Sciex 4000QTrap Pro LCMS equipped with a

C18 column in positive-ESI mode.

All analytical HPLC chromatography was carried out on a Shimadzu analytical HPLC system which utilized LC-10AD pumps, a SPD-10A UV-Vis detector, and a SCL-10A controller. A Shimadzu Shim-pack™ VP-ODS C18 analytical column (4.6 μ m pore size, 150 \times 4.6 mm) was used in these separations. Beginning with 100% Buffer A, a 1.4 mL/min gradient elution increase of 1% Buffer B/min for 50 min was used for all peptide chromatograms (Buffer A = 0.1% TFA/H₂O; Buffer B = 0.1% TFA/ACN). Peptide elution profiles were detected at 214 nm and 254 nm.

5.2 Synthetic Procedures

Synthesis of 2.

In an oven dried flask, **1** (10.07 g, 29.49 mmol) was dissolved in THF (120 mL) under an atmosphere of N₂. *N*-hydroxysuccinimide (3.77 g, 32.76 mmol) was added and the solution was cooled to 4 °C. Once cooled, DCC (6.77 g, 32.81 mmol) was added and the reaction was allowed to proceed at 4 °C for 1 h and then at room temperature for an additional 5 h. Thereupon, the reaction mixture was filtered and the filtrate was evaporated *in vacuo*. The resulting residue was dissolved in 200 mL dichloromethane and transferred to a separatory funnel. The organic layer was extracted with aqueous saturated NaHCO₃ solution (1 x 100 mL) and H₂O (1 x 100 mL), then washed with brine (1 x 100 mL). The organic layer was dried over MgSO₄, filtered, and concentrated *in vacuo*. The crude product was recrystallized from Et₂O. The crystals were washed with cold Et₂O (6 x 15 mL) and dried *in vacuo* to yield **2** (12.41 g, 96.0%) as a white, crystalline solid.

R_f = 0.27 (1:1 hexane/ethyl acetate). ¹H NMR (500 MHz, Chloroform-*d*) δ 11.11 (br s, 1H), 7.21 (d, *J* = 8.7 Hz, 2H), 6.83 (d, *J* = 8.6 Hz, 2H), 5.33 (d, *J* = 8.0 Hz, 1H), 4.54 (dd, *J* = 7.1, 6.6 Hz, 1H), 3.78 (s, 3H), 3.69 (s, 2H), 2.91 (dd, *J* = 14.1, 5.9 Hz, 1H), 2.85 (dd, *J* = 14.1, 5.9 Hz, 1H), 1.45 (s, 9H). ¹³C NMR (125 MHz, CDCl₃) δ 175.81, 158.76, 155.49, 130.07, 129.54, 114.03, 80.55, 77.31, 77.06, 76.80, 55.26, 52.97, 36.09, 33.19, 28.31. MS (pos APCI) *m/z* 339.9 [(M – Boc + H)⁺, calculated for C₂₀H₂₆N₂O₇S: 438.15].

Synthesis of 3.

In an oven dried flask, glycolic acid (1.25 g, 16.42 mmol) was dissolved in THF (87 mL) under an atmosphere of Ar. Then pyridine (1107 μ L, 13.68 mmol), DMAP (187 mg, 1.53 mmol), and **2** (6.02 g, 13.68 mmol) were added and the reaction was heated to 66 °C and subsequently refluxed for 24 h. The reaction mixture was concentrated *in vacuo*. The resulting residue was dissolved in ethyl acetate (80 mL) and transferred to a separatory funnel with 10% aqueous citric acid solution (80 mL). The organic layer was separated and extracted with aqueous saturated NaHCO₃ solution (1 x 80 mL). The combined aqueous layers were acidified to pH 2.5 with 12 N HCl. The acidified aqueous layer was back extracted with ethyl acetate (2 x 80 mL). The combined organic layers were washed with brine (1 x 150 mL), dried over MgSO₄, filtered, and concentrated *in vacuo* to yield **3** (5.29 g, 96.8%) as a white-yellow foam, which was immediately used in the synthesis of **5**.

Synthesis of 5.

In a round bottom flask, **3** (1.03 g, 2.57 mmol) was dissolved in 1:1 TFA/DCM (25 mL) and the mixture was stirred for 1 h at room temperature with ventilation. Upon reaction completion (monitored by TLC, 9:1 acetone/MeOH), the solvent was concentrated *in vacuo*. The resulting residue was repeatedly dissolved in methanol with subsequent concentration *in vacuo* (to remove residual TFA) to yield **4** (100% yield assumed) as an orange foam, which was used without further purification in subsequent steps.

In a round bottom flask, **4** (2.57 mmol assumed from previous step) was dissolved in 1,4-dioxane (7.5 mL) and a solution of NaHCO₃ (647 mg, 7.7 mmol) in H₂O (12.5 mL) was added to the mixture. The solution was cooled to 4 °C and a solution of Fmoc-OSu (1.56 g, 4.62 mmol) in 1,4-dioxane (5 mL) was added dropwise over 30 min via syringe. The mixture was stirred for 1 h at 4 °C. After 1 h, additional 1,4-dioxane (25 mL) was added to fully dissolve all solids. The pH of the reaction mixture was adjusted to 8 via the addition of aqueous saturated NaHCO₃ solution. Once these conditions were achieved, the mixture was stirred for 24 h at r.t. The mixture was transferred to a separatory funnel with H₂O (100 mL). The aqueous layer was extracted with ethyl acetate (2 x 100 mL). The organic layer was back extracted with aqueous saturated NaHCO₃ solution (1 x 100 mL). The combined aqueous layers were acidified to a pH of 1 with 12 N HCl and extracted with ethyl acetate (3 x 100 mL). The combined organic layers were dried over MgSO₄ and concentrated *in vacuo*. The resulting residue was purified via flash chromatography (100% dichloromethane → 9:1 dichloromethane/MeOH) to yield **5** (1.16 g, 80.4%) as a white solid.

$R_f = 0.20$ (9:1 dichloromethane/MeOH). $^1\text{H NMR}$ (500 MHz, Chloroform-*d*) δ 7.76 (d, $J = 7.2$ Hz, 2H), 7.60 (t, $J = 6.6$ Hz, 2H), 7.39 (t, $J = 7.4$ Hz, 2H), 7.31 (t, $J = 7.4$ Hz, 2H), 7.20 (d, $J = 8.3$ Hz, 2H), 6.83 (d, $J = 8.4$ Hz, 2H), 5.55 (d, $J = 7.8$ Hz, 1H), 4.72 (m, 2H), 4.64 (m, 1H), 4.41 (d, $J = 7.0$ Hz, 2H), 4.23 (t, $J = 6.9$ Hz, 1H), 3.76 (s, 3H), 3.69 (s, 2H), 2.98 (dd, $J = 14.0, 6.5$ Hz 1H), 2.86 (dd, $J = 14.0, 6.5$ Hz, 1H) (CO_2H not observed). $^{13}\text{C NMR}$ (125 MHz, CDCl_3) δ 170.96, 170.39, 158.97, 156.11, 143.76, 141.46, 130.20, 129.48, 127.92, 127.26, 125.24, 120.17, 114.21, 77.41, 77.16, 76.91, 67.54, 60.99, 55.41, 53.50, 47.22, 36.22, 33.31. MS (pos ESI) m/z 522.3 $[(\text{M} + \text{H})^+]$, calculated for $\text{C}_{28}\text{H}_{27}\text{NO}_7\text{S}$: 521.15].

Figure 10. ^1H NMR spectrum of **1** in CDCl_3 .

Figure 11. ^{13}C NMR spectrum of **1** in CDCl_3 .

Figure 12. ^1H NMR spectrum of **2** in CDCl_3 .

Figure 13. ^{13}C NMR spectrum of **2** in CDCl_3 .

Figure 14. Positive ESI mass spectrum of **2**.

Figure 15. ^1H NMR spectrum of **5** in CDCl_3 .

Figure 16. ^{13}C NMR spectrum of **5** in CDCl_3 .

Figure 17. Positive ESI mass spectrum of **5**.